



HAL
open science

Role of circulation in European heatwaves using flow analogues

Aglaé Jézéquel, Pascal Yiou, Sabine Radanovics

► **To cite this version:**

Aglaé Jézéquel, Pascal Yiou, Sabine Radanovics. Role of circulation in European heatwaves using flow analogues. 2016. hal-01373903v1

HAL Id: hal-01373903

<https://hal.science/hal-01373903v1>

Preprint submitted on 29 Sep 2016 (v1), last revised 9 Nov 2017 (v2)

HAL is a multi-disciplinary open access archive for the deposit and dissemination of scientific research documents, whether they are published or not. The documents may come from teaching and research institutions in France or abroad, or from public or private research centers.

L'archive ouverte pluridisciplinaire **HAL**, est destinée au dépôt et à la diffusion de documents scientifiques de niveau recherche, publiés ou non, émanant des établissements d'enseignement et de recherche français ou étrangers, des laboratoires publics ou privés.

1 Role of circulation in European heatwaves using flow analogues

2 Aglaé Jézéquel · Pascal Yiou · Sabine Radanovics

3
4 Received: September 22, 2016/ Accepted:

5 **Abstract** The intensity of European heatwaves is connected to specific synoptic atmospheric circulation.
6 Given the relatively small number of observations, estimates of the connection between the circulation
7 and temperature require ad hoc statistical methods. This can be achieved through the use of analogue
8 methods, which allow to determine a distribution of temperature conditioned to the circulation.
9 The computation of analogues depends on a few parameters. In this article, we evaluate the influence of
10 the variable representing the circulation, the size of the domain of computation, the length of the dataset,
11 and the number of analogues on the reconstituted temperature anomalies. We tested the sensitivity of
12 the reconstitution of temperature to these parameters for four emblematic recent heat waves : June
13 2003, August 2003, July 2006 and July 2015. The paper provides general guidelines for the use of flow
14 analogues to investigate European summer heat waves. We found that Z500 is better suited than SLP
15 to simulate temperature anomalies, and that rather small domains lead to better reconstitutions. The
16 dataset length has an important influence on the uncertainty. We conclude by a set of recommendations
17 for an optimal use of analogues to probe European heatwaves.

18 **Keywords** Heatwaves, Europe, Atmospheric circulation

19 1 Introduction

20 There have been many studies showing that heatwaves are bound to become more intense and more
21 frequent under climate change (Field and Intergovernmental Panel on Climate Change 2012). The evo-
22 lution of the probabilities of those events and of their properties, such as intensity, duration and extent,

Aglaé Jézéquel
LSCE, CEA Saclay l'Orme des Merisiers, UMR 8212 CEA-CNRS-UVSQ, U Paris-Saclay, IPSL, Gif-sur-Yvette, France
Tel.: +33-169081142
Fax: +33-169087716
E-mail: aglae.jezequel@lsce.ipsl.fr

Pascal Yiou
LSCE, CEA Saclay l'Orme des Merisiers, UMR 8212 CEA-CNRS-UVSQ, U Paris-Saclay, IPSL, Gif-sur-Yvette, Franc

Sabine Radanovics
LSCE, CEA Saclay l'Orme des Merisiers, UMR 8212 CEA-CNRS-UVSQ, U Paris-Saclay, IPSL, Gif-sur-Yvette, Franc

is a key question for adaptation due to their impacts, including on crop yields (Ciais et al 2005) and human health (Peng et al 2011; Fouillet et al 2006). A first step is to understand the physical processes at play during heat waves, such as the influence of soil moisture (Seneviratne et al 2010), or SST (Feudale and Shukla 2007). Yiou and Nogaj (2004) studied the relation between the atmospheric circulation and extreme events over the North Atlantic and Horton et al (2015) linked the increase of heatwaves to the increase of the frequency of mainly anticyclonic weather types. In this paper, we aim at quantifying the role of the atmospheric circulation during spells of high temperatures, that occurred in major European heat waves. In particular, we want to understand which proportion of the heat wave intensities can be explained solely based on the associated atmospheric circulation, in an effort to disentangle its contribution compared to other factors (Shepherd 2015).

Our methodology is based on flow analogues (e.g. Yiou et al 2014). Historically, analogues were used in weather forecasting (e.g. Lorenz 1969; Duband 1981; Toth 1991a; Chardon et al 2016; Ben Daoud et al 2016). They have been used in empirical downscaling (e.g. Chardon et al 2014; Zorita and von Storch 1999), circulation dependent bias correction (e.g. Turco et al 2011; Hamill and Whitaker 2006; Hamill et al 2015; Djalalova et al 2015), in combination with ensemble data assimilation (Tandeo et al 2015), in probabilistic wind energy potential estimation (Vanvyve et al 2015), and paleo climate reconstruction (Schenk and Zorita 2012; G  mez-Navarro et al 2014).

Here, they are defined as days with an atmospheric circulation similar to the day of interest, with the assumption that circulation is connected to a climate variable such as temperature. They allow us to isolate certain types of circulation and to measure their influence on the temperature. We then compare the probability density functions of temperature anomalies reconstructed for both randomly picked days and days picked among analogues. The analogues depend on many parameters, including the size of the domain of computation, or the length of the dataset. The goal of this paper is to provide general guidelines to choose those parameters to get flow analogues adapted to the study of European summer heatwaves. Those guidelines are obtained from four emblematic cases of heatwaves. A former study of Toth (1991b) focused on the distance to minimize for obtaining analogues. Van Den Dool (2007) provided tests of predictability based on analogues. Our paper includes physical parameters on which the analogues are computed, and focuses on temperature reconstructions.

Section 2 details the methodology used in this study. Section 3 tests the sensitivity of several physical and statistical parameters on which the methodology is based. A part of this section is devoted to a qualitative evaluation of the uncertainty related to the limited size of the datasets. Section 4 focuses on the role played by the circulation in each of the chosen case studies. The results are discussed in Section 5 and conclusions appear in Section 6.

2 Methodology

2.1 Heat wave selection

We focus on summer heat waves, knowing that the processes involved in the development of a heat wave vary from one season to the other. We focus on warm months (June–July–August: JJA). We chose heatwaves that stroke Europe since 2000: June and August 2003 (e.g. Beniston and Diaz 2004; Fischer

65 et al 2007; Cassou et al 2005; Stéfanon et al 2012) in Western Europe (WE), July 2006 (Rebetez et al
66 2009) in Northern Europe (NE), and July 2015 (Russo et al 2015) in Southern Europe (SE). We use the
67 NCEP reanalysis I dataset (Kalnay et al 1996), which provides us with 68 years of data from 1948 to
68 2016. The advantage of this dataset is that it is updated near real time (with a three days delay), so that
69 the methodology could give results already a few days after a given event. Longer datasets like ERA20C
70 (Poli et al 2016) or the NCEP 20th Century Reanalysis (Compo et al 2011) are less frequently updated
71 or do not include 2015, and were therefore not retained.

73 The peak temperatures occurred in different regions for each heatwave. These regions correspond to the
74 black boxes in figure 1. They are centered on the region of highest temperature anomaly. The size of
75 the boxes was defined such that the monthly temperature anomalies averaged over them are records
76 (see figure 2). Hence we identify two heatwaves in 2003, in June and August, which is consistent with
77 (Stéfanon et al 2012). Choosing a slightly larger box does not alter the results or the methodology.

78

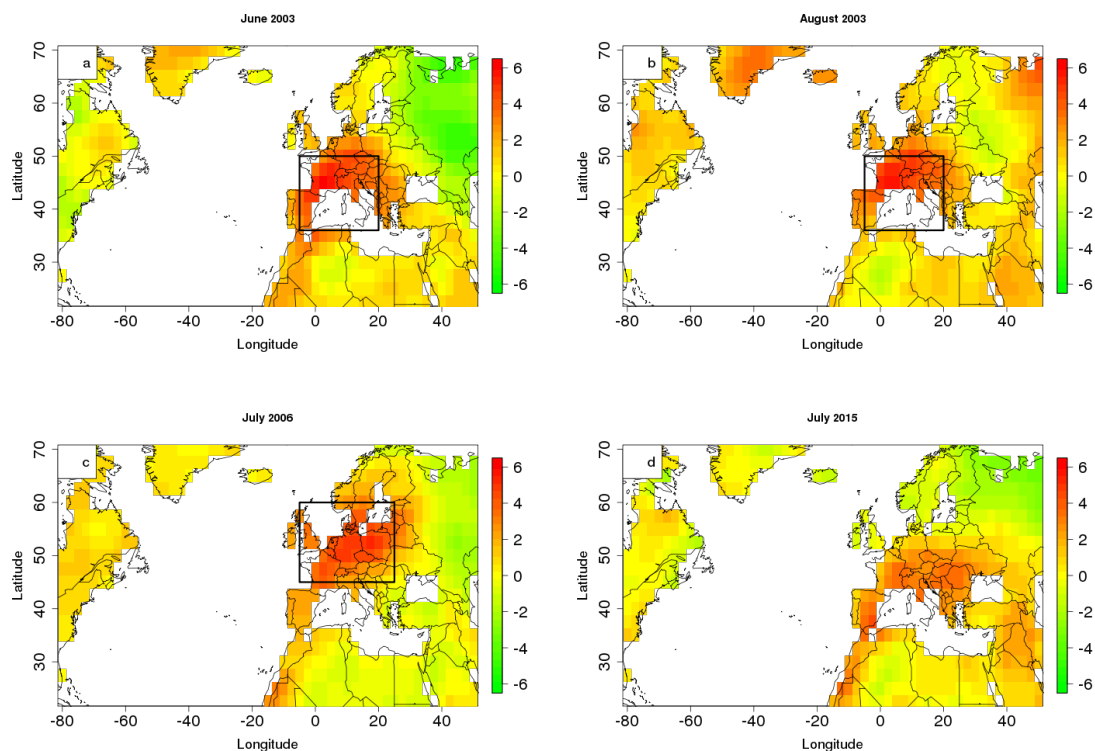


Fig. 1: Monthly mean land temperature anomalies (NCEP dataset with reference to the 1948-2015 mean) for the four case studies (in C). The black rectangles indicate the regions of interest for the rest of the study.

79 We observe a significant linear trend ($p - value < 0.05$), related to climate change, for each month and
 80 region studied (red lines in figure 2): 0.23 C per decade for June (WE), 0.24 C for July (NE and SE) and
 81 0.25 C for August(WE). For the rest of the study we calculate detrended temperatures using a non-linear
 82 trend, calculated with a cubic smoothing spline (green lines in figure 2). The reason is to extract the
 83 role of circulation in high temperature extremes, regardless of the state of the background climate, the
 84 evolution of which is non-linear.

85

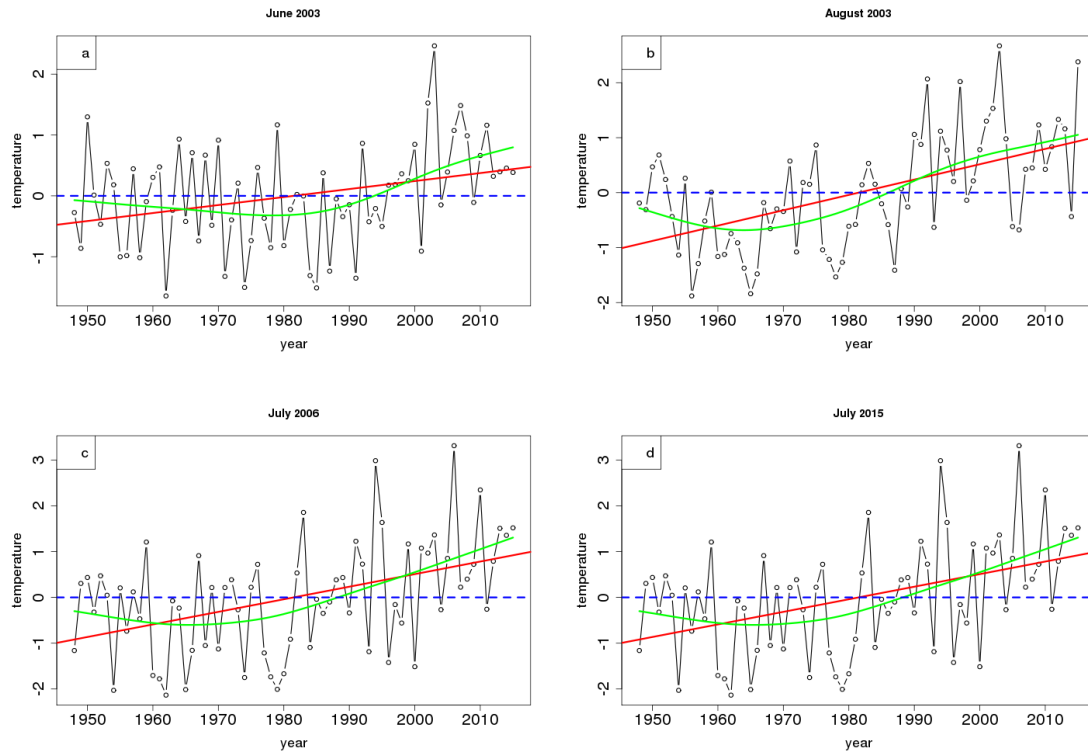


Fig. 2: Evolution of the monthly temperature anomalies averaged over the regions defined in figure 1. The red line corresponds to the linear trend, which is significant ($p - value < 0.05$). The green line corresponds to a non linear trend calculated with a cubic smoothing spline.

86 2.2 Flow analogues

87 We used flow analogues to extract the contribution of circulation dynamics to the chosen heat wave
 88 events comparing their temperature anomalies to those of analogues. Analogues were defined as the N
 89 days with the most similar sea level pressure (SLP) or geopotential height at 500 hPa (Z500) fields. The

90 similarity was measured with the Euclidean distance between two maps (Yiou 2014). We only considered
 91 the days within a 61 calendar days (30 days before and 30 days after) window centered on the day of
 92 interest because of the seasonal cycle of both circulation and temperature (Yiou et al 2012). We fur-
 93 ther exclude the days coming from the same year as the event from the 1948–2015 data set, because
 94 of the persistence of the circulation. The program used to compute analogues CASTf90 is available
 95 online (<https://a2c2.lsce.ipsl.fr/index.php/licences/file/castf90?id=3>). Once the analogues
 96 were selected, we took the observable of interest (the detrended temperature) on those selected days.
 97 The whole process is summarized in figure 3.
 98

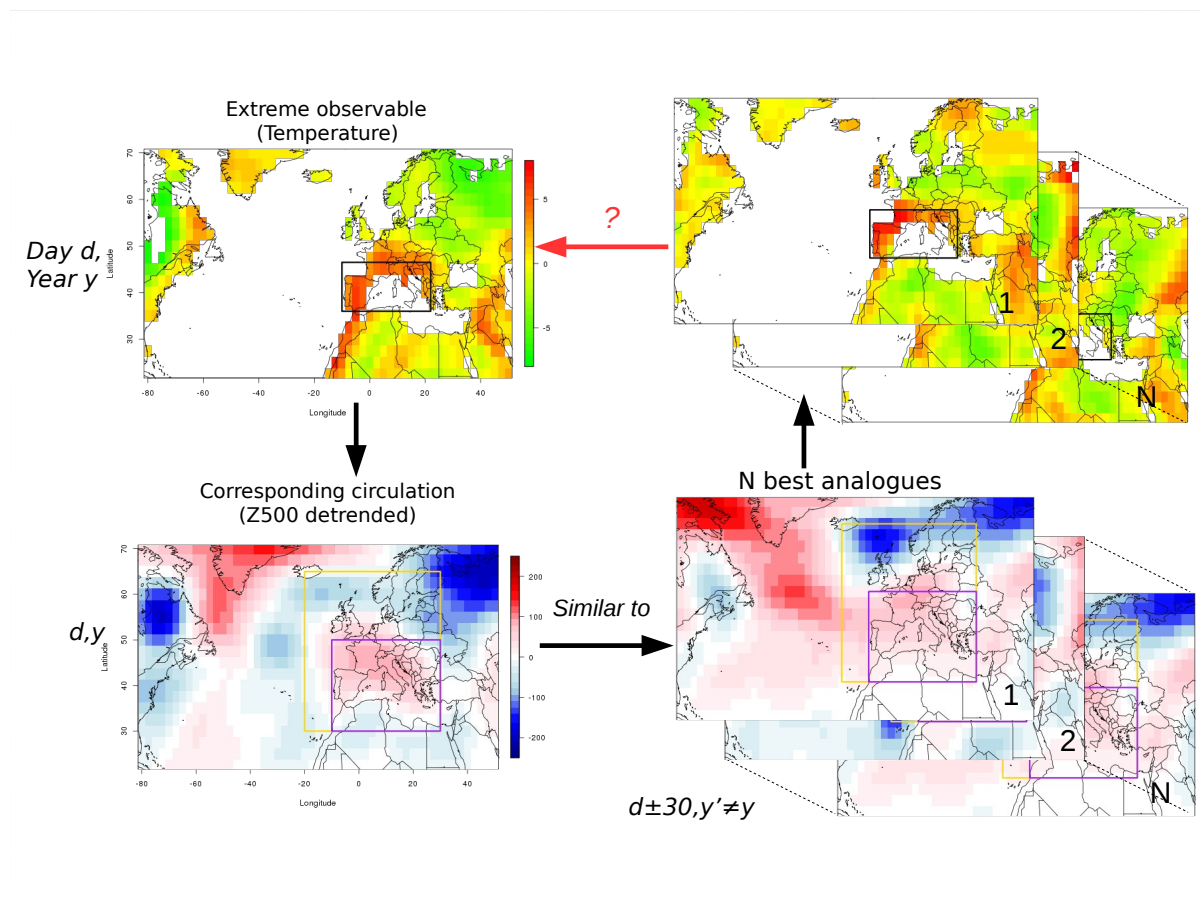


Fig. 3: A day with an extreme temperature (map on the top left) has a corresponding circulation, represented by the geopotential at 500 hPa (map on the bottom left). Flow analogues are days within the database which have a similar circulation to the day of interest (maps on the bottom right). The temperatures of the analogues (maps on the top right) are then compared to the temperature of the day of interest (map on the top left).

Days of the event	Corresponding analogues	Randomly picked analogue
01/07/2015	$\text{ana}_1^1, \text{ana}_1^2, \dots, \text{ana}_1^N$	ana_1^i
02/07/2015	$\text{ana}_2^1, \text{ana}_2^2, \dots, \text{ana}_2^N$	ana_2^i
\vdots	\vdots	\vdots
31/07/2015	$\text{ana}_{31}^1, \text{ana}_{31}^2, \dots, \text{ana}_{31}^N$	ana_{31}^i

Table 1: Simulation of uchronic months using randomly picked analogues for July 2015.

99 2.3 Reconstruction of temperature distributions

100 The goal is to reconstruct the probability distribution of temperature conditional to the atmospheric
101 circulation. For this, we consider a day i , with a temperature T_i and a circulation C_i with N analogues
102 $C_i^1 \dots, C_i^N$. The circulation analogues $\text{ana}_i^1 \dots \text{ana}_i^N$ provide N copies of the temperature. Hence, for
103 each day, we can randomly pick one of the N best analogues, in order to recreate a sequence of temper-
104 atures over a month. Its resulting mean temperature will be called *uchronic*, because it is a temperature
105 that might have been for a given circulation pattern sequence. By reiterating this process, we recre-
106 ate probability distributions of uchronic monthly detrended temperature conditional to the atmospheric
107 circulation. We then compare this distribution to a distribution built from random days instead of ana-
108 logues. In the rest of the article, we set the number of random iterations to 1000. This procedure is a
109 simplified version of the stochastic weather generator of Yiou (2014), who also used weights based on
110 the distances of the analogues. Table 1 illustrates this process for the July 2015 case.

111
112 In order to measure the contribution of the circulation we compared the distribution of uchronic temper-
113 ature anomalies with a control distribution built using random days. However, the variability of random
114 summers built that way is not realistic because the dependence between consecutive days is not accounted
115 for. Analogues are by construction dependent from one another, because they are calculated using maps
116 from following (hence correlated) days. Randomly picked days are independent.

117
118 In order to create a more realistic distribution of temperature using random days, we also calculated
119 means by using only one out of M days. M is an assessment of the persistence of the circulation. We
120 computed the autocorrelation of the detrended Z500 NCEP dataset for summer months (JJA) on each
121 of the four small domains, for each grid points, with lags from 1 to 20 days (similar to Yiou et al (2014)).
122 For more than 10 days, the autocorrelations median tends to an asymptotic value of approximately 0.1.
123 For three days, the median of the autocorrelation distribution is of approximately 0.65. For four days,
124 it decreases to 0.45. Since the regions are small, the number of degrees of freedom is small too, which
125 means that an autocorrelation of 0.45 is negligible. We hence arbitrarily decided to set $M=3$. This is
126 probably an underestimation for events alike the ones studied here with a long-lasting blocking situation.

128 3 Parameter sensitivity tests

129 The presented method depends on a few parameters. Their choice has an influence on both the results
130 and their robustness. The following section explores the role of those parameters and how tuning them
131 may give us further information on the relationship between circulation patterns and extreme tempera-
132 ture. We also want to know whether those parameters should depend on the specific event or not. This

133 determines how general the approach can be and therefore its potential application to future events and
 134 other extra-tropical regions. In particular, we studied the role played by physical parameters: the variable
 135 on which we compute analogues (SLP vs. Z500), the choice of the size of the domain on which we compute
 136 analogues, and the length of the dataset, and a statistical parameter: the number N of analogues we kept.
 137

138 3.1 Variable representing the circulation

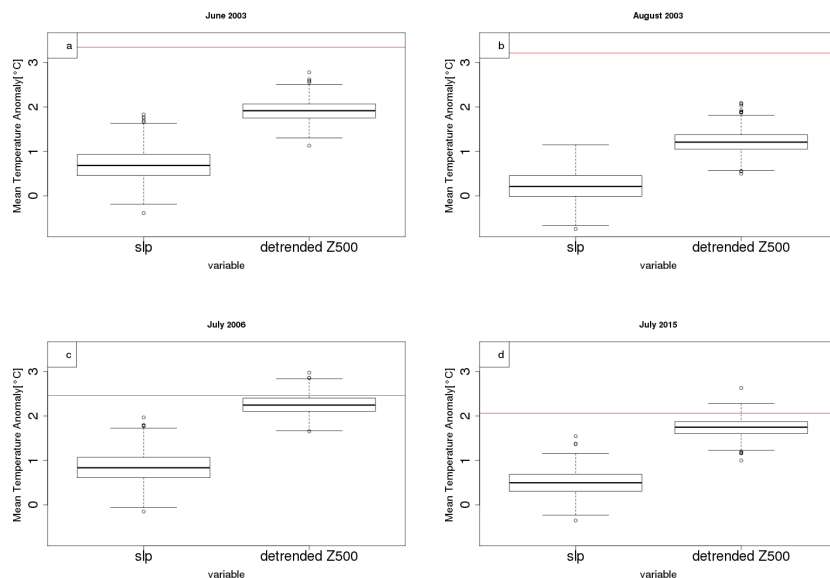


Fig. 4: Dependence of the probability density on the variable representing circulation. Difference between analogues generated distributions calculated using SLP (left boxplot of each subfigure) or detrended geopotential height at 500 hPa (right boxplot of each subfigure) for each case study: June 2003 (a), August 2003 (b), July 2007 (c), July 2015 (d). The red line represents the observed detrended temperature anomaly of the event.

139 SLP (e.g. Cassou and Cattiaux 2016; Sutton and Hodson 2005; Della-Marta et al 2007) and Z500 (e.g.
 140 Horton et al 2015; Quesada et al 2012; Dole et al 2011) are the most commonly used variables to study
 141 the atmospheric circulation. We calculated analogues using either the SLP or the detrended Z500. The
 142 detrending was needed due to the dependence of Z500 on lower tropospheric temperatures, which are
 143 increasing due to anthropogenic climate change. The detrending was done for the mean field using a
 144 nonlinear trend. The resulting uchronic temperature anomalies for each event are shown in figure 4.
 145 The analogues computed using Z500 give results closer to the actual anomaly of the event than those
 146 computed using SLP. This is probably related to the heat low process (e.g. Portela and Castro 1996).
 147 Warm anomalies of surface temperature lead to convection. The elevation of warm air masses creates a

148 local depression, which adds on top of an anticyclonic anomaly a cyclonic anomaly. This flattens the SLP
149 patterns and blurs the signal, which does not happen with Z500. By using Z500 we also avoid any in-
150 fluence of the relief. Hence, we keep the detrended Z500 to compute the analogues for the rest of the study.

151

152 3.2 Size of the domain

153 The scale on which we compare circulation patterns plays a key role in the computation of the analogues.
154 If the domain is too large, the system becomes too complicated, with too many degrees of freedom. The
155 analogues could consequently only extract a low frequency signal, like the seasonal cycle. Van den Dool
156 (1994) evaluates that it would take 10^{30} years of data to find two matching observed flows for analogues
157 computed over the Northern Hemisphere. If we choose too small a domain, then we cannot study the role
158 of the synoptic circulation. So, on the one hand, it is no use to calculate analogues on whole hemispheres,
159 and on the other hand, we do not want to select domains which are smaller than the typical scale of
160 extra-tropical cyclones (1000 km approximately). Radanovics et al (2013) investigated automatic algo-
161 rithms to adjust the domain size of the analogues for precipitation. Here, we prefer to select a domain
162 that yields an a priori physical relevance to account for the most important features of the flow that
163 affects high temperatures in Europe.

164

165 The ideal size of the domain reveals the scale at which the processes are relevant and may very well vary
166 from one event to the other. This especially applies for studies on other types of events such as heavy
167 precipitation, droughts or storms. We compared three different domains shown in figure 5 (right hand
168 side):

- 169 – a large domain (the whole maps in figure 5), including the North Atlantic region, which corresponds
- 170 to the domain usually used to calculate weather regimes (Vautard 1990; Michelangeli et al 1995),
- 171 – a medium domain (the golden rectangles in figure 5), centered on Europe, which is much smaller than
- 172 the North Atlantic domain while being common to all events, and
- 173 – a small domain tailored for each event (the purple rectangles in figure 5), depending on the circulation
- 174 pattern of the specific summer .

175 The results are displayed on the left hand side of figure 5. The event of interest, shown by the red lines, is
176 better reproduced for the smaller domains. This is because there are circulation patterns included in the
177 North Atlantic domain which probably play no role in the establishment of a heat wave over Europe. For
178 example in July 2015 we observe an important anticyclonic anomaly over Greenland. It adds a constraint
179 on the analogues while supposedly playing no role on the lesser anticyclonic anomaly over the Northern
180 Mediterranean region. The standard deviation also decreases with the size of the domain.

181

182 It is relevant to rely on standard domains for a first estimation of the role played by the circulation in
183 the occurrence of a heat wave, for example by using the regions defined in Field and Intergovernmental
184 Panel on Climate Change (2012). However, for a finer analysis focused on one specific heatwave, or a few
185 given events, the choice of a tailored small domain will give better results. In the rest of the study, we
186 hence kept the smaller domains.

187

3.3 Length of the dataset

The NCEP dataset contains 68 years. Although the recombination of analogues allows to recreate new events, the dataset is finite and hence does not cover the whole range of possible events. For example, if the circulation leading to a heat wave has a return period of more than the dataset length, there might not be the like of it in the dataset. Furthermore, even if there are close daily analogues to the daily circulation of the event, it might not account for other thermodynamical processes that may or may not happen simultaneously and lead to extreme temperatures. This shortcoming is called sampling uncertainty (Committee on Extreme Weather Events and Climate Change Attribution 2016, Chap. 3), related to the fact that the past is one occurrence of many realizations which could have happened for a given state of the climate.

In order to get an order of magnitude of that uncertainty in the reconstruction of probability densities of temperature we used a 500 years long pre-industrial run from CMIP5 (Taylor et al 2012). The model used is GFDL-ESM2M (Dunne et al 2012, 2013). We chose this model because it was the model available on the IPSL data center with the longest run for both the temperature and the Z500. We selected one heat wave similar to July 2015, both in terms of temperature anomaly (compared to the detrended anomaly of July 2015) and circulation patterns (see figure 6). We assume that the internal variability of the model is similar to the internal variability of the reanalysis.

Analogues were computed for 60 different subsets of the 500 year dataset. The lengths of the subsets are 33, 68, 100 and 200 years (e.g. subsets of 68 consecutive years each, starting every 5 years of the data set). We then compared the means of reconstructed distributions to one another for a given subset length. The difference between the maximum and minimum means calculated this way gives an estimation of the uncertainty related to the limited length of the dataset.

Figure 7 displays the results for subsets of 33, 68, 100 and 200 years. When the number of years of the subset decreases, the variability increases, going up to approximately 0.71 C for the 33 years subsets, 0.62 C for 68 years, 0.36 C for 100 years, and 0.14 C for 200 years. This information is precious to determine in which measure smaller datasets are relevant for this methodology. It also proves that dividing the NCEP dataset in two smaller periods of 33 years is not enough to attribute the difference between the two to climate change, rather than to natural variability. Indeed, the internal variability between the two periods would be of the same order of magnitude than the difference caused by climate change.

The ability to find analogues close to the circulation of interest is related to both the size of the dataset and the size of the domain on which the analogues are computed (Van den Dool 1994). It means that the analogues method will get more and more accurate as the reanalysis dataset extends in the years to come.

3.4 Number of analogues

For the reconstruction of events by recombination of analogues, we kept the N best analogues. The choice of N has an influence on both the reconstructed anomalies of temperature and the statistical robustness of the study. The best analogues temperature anomalies are closer to the temperature anomalies of the actual events for all case studies (see figure 8). We need to find a trade-off between having the best ana-

Event	Observed detrended temperature	Mean detrended uchronic temperature
06/2003	3.3 C	1.9 C
08/2003	3.2 C	1.2 C
07/2006	2.5 C	2.3 C
07/2015	2.1 C	1.7 C

Table 2: Observed detrended temperature compared to the mean detrended uchronic temperature for each case study.

logues which give results closer to both the observed circulation and temperature anomaly, and having enough analogues to create a robust distribution. The difference of temperature mean between keeping 5 and 30 analogues is of less than 0.2 C, so the sensitivity on this parameter is rather low. We kept 20 analogues for the rest of the study.

234

235 4 The role of circulation in heat waves

236 With the parameters kept (Z500, small domains, 68 years reanalysis data, and 20 analogues) we simulated
 237 1000 uchronic monthly mean temperature anomalies for each of the four selected heatwave events (see
 238 the analogues boxplots in figure 9). The circulation contribution corresponds to the mean of the uchronic
 239 temperature distribution. The spread of the boxplots is due to the range of other processes which can, for
 240 a given circulation, lead to different temperatures. The control boxplots correspond to randomly picked
 241 days. The control with dependence boxplots correspond to randomly picked days using only one out of
 242 three days. The circulation during heat waves corresponds to a long-lasting blocking situation, hence the
 243 persistence is probably more than three days. This underestimation, combined with the limited length of
 244 the dataset explains why the studied events are all outside of the distribution calculated using random
 245 days.

246

247 For every events, the circulation plays a significant role in the occurrence of the extreme. It only explains
 248 a part of it, more or less significant depending on the event. Indeed, it explains 38% of the anomaly for
 249 August 2003, 57% for June 2003, 81% for July 2015 and 92% for July 2006 (see table 2). The standard
 250 deviation of the analogues distribution is also systematically lower than both the random ones, and ap-
 251 proximately a third of the one taking into account the persistence of the circulation. Using this approach
 252 is equivalent to zooming on a specific part of the distribution conditioned to the flow.

253

254 In order to contextualize the four case studies, we reproduced the same kind of probability density func-
 255 tion experiments for the same regions from 1948 to 2015 (figure 10). This type of recontextualisation can
 256 be interpreted as an estimation of how extreme an event really is, as regards to its atmospheric circulation.

257

258 The observed month falls between the tenth and ninetieth percentiles of the analogues distribution for
 259 more than half of the years and between the first and ninety-ninth percentiles for more than two thirds of
 260 the years, even though the analogue distribution has a small spread compared to the total distribution.
 261 The years out of the 98% interval correspond mostly to important anomalies of temperature (absolute
 262 value > 0.5 C). Less than a quarter of the years have different signs of anomaly between the real event
 263 and the mean of the analogue distribution. Those years correspond to small anomalies of temperature

(absolute value < 0.5 C).

5 Discussion

The median of the uchronic distribution is generally different from the observed temperature. In some cases, the observed anomaly (red line on figure 9) is not even in the uchronic distribution. On figure 9 for June and August 2003, and for some of the years on figure 10, this is the case (indeed, the monthly detrended anomaly for both months are of more than 3 C). This difference shows caveats in the methodology, and that heatwave events cannot be explained only by its circulation.

Flow analogues are unable to take into account the role played by the soil-moisture feedback. Indeed, the analogues do not take into account the history of the heat wave. Extreme heat waves happen when the circulation causing the initial anomaly of temperature lasts more than a few days. As soil moisture becomes limited, the cooling of the atmosphere through evapotranspiration gets weaker, which exercises a positive feedback on the temperature. Seneviratne et al (2010) isolates a dry and a wet regime, with a transition phase between both. The three regions used here are prone to different evaporative regimes. In particular, the Northern Europe region is wetter than the other two. The role of soil moisture is thus less important (Seneviratne et al 2006). On the other hand, several articles (Stéfanon et al 2012; Fischer et al 2007) showed the role of soil moisture in the exceptional temperature anomalies of summer 2003, especially for August. The analogues are picked without any condition on the previous days, and consequently they fail to reach the observed anomaly.

The main caveat of this methodology is the limited size of the dataset, which introduces an important sampling uncertainty, as seen in section 3.3, and also affects the quality of the analogues. As a result, the analogues might not be good enough to accurately reproduce the dynamical contribution. Indeed, an extreme temperature can be related to a rare circulation, which might not be found in a short dataset. The distances between the analogues and the event, as well as their correlations, are indices to evaluate the relevance of the analogues in each case. A better definition of what is a good analogue will require further studies. Depending on the magnitude of the studied event, it might not be possible to reconstruct a comparable month by resampling the days in the dataset. This is the case for both June and August 2003, which have temperature anomalies about one degree Celsius above all the other years, despite the detrending. If the event is too rare, it will not be possible to reconstitute uchronic temperature close to the observed one.

Another limitation relates to the coherence of the uchronic summers computed using analogues. Due to the persistence of the circulation, the analogues we picked for each day might be correlated to one another. In fact, when we compare the analogues sample of 20 times the number of days of the month we want to study, only half of the analogues are unique. However, the persistence is still underestimated compared to real summers. Consequently, the spread of the computed distributions is underestimated.

6 Conclusion

This paper proposes to quantify the role of the atmospheric circulation in the occurrence of an extreme monthly anomaly of temperature. The strength of our methodology is that it is easily adaptable to other regions, and to other events. The parameter sensitivity tests of section three provide general guidelines to choose flow analogues to investigate European summer heatwaves. It is best to use detrended Z500 as a proxy of circulation, and to compile the analogues on a small domain centered on the Z500 anomaly concomitant to the event. We also advise to use as long a dataset as possible.

The results on parameter sensitivities have potential implications for applications of the analogue method in a downscaling or reconstruction context as well. The questions of the predictor variable (or variables), that is the circulation proxy, is relevant in the downscaling context but may vary depending on the predictand variable. The question of domain size has been treated by several authors (e.g. Chardon et al 2014; Radanovics et al 2013; Beck et al 2015) and the results are systematically in favor of relatively small domains, in line with our findings. Tests on archive lengths larger than typical reanalysis record lengths are rarely performed. The results are relevant since split-sample validation of downscaling methods is common practice and our results show that splitting the limited length reanalysis record leads to large uncertainties in the uchronic temperatures due to the limited sample size even using a relatively small domain.

The reconstitution of an ensemble of uchronic temperatures for a given circulation is a first step in refining Cattiaux et al (2010)'s approach to extreme event attribution. Indeed, looking at changes for a given circulation should reduce the signal to noise ratio of climate change versus natural variability (Trenberth et al 2015) in what Shepherd (2016) calls a storyline approach to extreme events attribution. Since among the tested parameters only the regions of the temperature anomaly and the geopotential height field depend on the event, a diagnosis on heat waves can be automatized and computed in less than a day once the data set is available. This should allow to use the presented method in an operational way for example for conditional fast-track attribution of extreme events (Haustein et al 2016).

7 Acknowledgment

NCEP Reanalysis data provided by the NOAA/OAR/ESRL PSD, Boulder, Colorado, USA, from their Web site at <http://www.esrl.noaa.gov/psd/>.
Program to compute analogues available online <https://a2c2.lsce.ipsl.fr/index.php/licences/file/castf90?id=3>. PY and SR are supported by the ERC Grant A2C2 (No. 338965).

References

- Beck C, Philipp A, Jacobeit J (2015) Interannual drought index variations in Central Europe related to the large-scale atmospheric circulation—application and evaluation of statistical downscaling approaches based on circulation type classifications. *Theor Appl Climatol* 121(3):713–732, DOI 10.1007/s00704-014-1267-z
- Ben Daoud A, Sauquet E, Bontron G, Obled C, Lang M (2016) Daily quantitative precipitation forecasts based on the analogue method: Improvements and application to a French large river basin. *Atmos Res* 169:147–159, DOI 10.1016/j.atmosres.2015.09.015

- 343 Beniston M, Diaz HF (2004) The 2003 heat wave as an example of summers in a greenhouse climate? Observations and
344 climate model simulations for Basel, Switzerland. *Glob Planet Change* 44(1-4):73–81, DOI 10.1016/j.gloplacha.2004.
345 06.006
- 346 Cassou C, Cattiaux J (2016) Disruption of the European climate seasonal clock in a warming world. *Nat Clim Change*
347 (April):1–6, DOI 10.1038/nclimate2969
- 348 Cassou C, Terray L, Phillips AS (2005) Tropical atlantic influence on european heat waves. *J Clim* 18(15):2805–2811,
349 DOI 10.1175/JCLI3506.1
- 350 Cattiaux J, Vautard R, Cassou C, Yiou P, Masson-Delmotte V, Codron F (2010) Winter 2010 in Europe: A cold extreme
351 in a warming climate. *Geophys Res Lett* 37(20):1–6, DOI 10.1029/2010GL044613
- 352 Chardon J, Hingray B, Favre AC, Autin P, Gailhard J, Zin I, Obled C (2014) Spatial Similarity and Transferability of
353 Analog Dates for Precipitation Downscaling over France. *J Clim* 27(13):5056–5074, DOI 10.1175/JCLI-D-13-00464.1
- 354 Chardon J, Favre AC, Hingray B (2016) Effects of Spatial Aggregation on the Accuracy of Statistically Downscaled
355 Precipitation Predictions. *J Hydrometeor* 17(5):1561–1578, DOI 10.1175/JHM-D-15-0031.1
- 356 Ciais P, Reichstein M, Viovy N, Granier A, Ogee J, Allard V, Aubinet M, Buchmann N, Bernhofer C, Carrara A, Chevallier
357 F, De Noblet N, Friend AD, Friedlingstein P, Grunwald T, Heinesch B, Keronen P, Knohl A, Krinner G, Loustau D,
358 Manca G, Matteucci G, Miglietta F, Ourcival JM, Papale D, Pilegaard K, Rambal S, Seufert G, Soussana JF, Sanz
359 MJ, Schulze ED, Vesala T, Valentini R (2005) Europe-wide reduction in primary productivity caused by the heat and
360 drought in 2003. *Nature* 437(7058):529–533, DOI 10.1038/nature03972
- 361 Committee on Extreme Weather Events and Climate Change Attribution (2016) Attribution of Extreme Weather Events
362 in the Context of Climate Change. DOI 10.17226/21852
- 363 Compo GP, Whitaker JS, Sardeshmukh PD, Matsui N, Allan RJ, Yin X, Gleason BE, Vose RS, Rutledge G, Bessemoulin
364 P, Brönnimann S, Brunet M, Crouthamel RI, Grant AN, Groisman PY, Jones PD, Kruk M, Kruger AC, Marshall
365 GJ, Maugeri M, Mok HY, Nordli O, Ross TF, Trigo RM, Wang XL, Woodruff SD, Worley SJ (2011) The Twentieth
366 Century Reanalysis Project. *Quat J Roy Met Soc* 137:1–28, DOI 10.1002/qj.776.
- 367 Della-Marta PM, Luterbacher J, von Weissenfluh H, Xoplaki E, Brunet M, Wanner H (2007) Summer heat waves over
368 western Europe 1880–2003, their relationship to large-scale forcings and predictability. *Clim Dyn* 29(2-3):251–275,
369 DOI 10.1007/s00382-007-0233-1
- 370 Djalalova I, Delle Monache L, Wilczak J (2015) PM2.5 analog forecast and Kalman filter post-processing for the Community
371 Multiscale Air Quality (CMAQ) model. *Atmos Environ* 108:76–87, DOI 10.1016/j.atmosenv.2015.02.021
- 372 Dole R, Hoerling M, Perlwitz J, Eischeid J, Pegion P, Zhang T, Quan XW, Xu T, Murray D (2011) Was there a basis for
373 anticipating the 2010 Russian heat wave? *Geophys Res Lett* 38(6):1–5, DOI 10.1029/2010GL046582
- 374 Van den Dool H (1994) Searching for analogues, how long must we wait? *Tellus A* 46(3):314–324
- 375 Duband D (1981) Prévision spatiale des hauteurs de précipitations journalières (A spatial forecast of daily precipitation
376 heights). *La Houille Blanche* (7-8):497–512, DOI 10.1051/lhb/1981046
- 377 Dunne JP, John JG, Shevliakova S, Stouffer RJ, Krasting JP, Malyshev SL, Milly PCD, Sentman LT, Adcroft AJ, Cooke
378 W, Dunne KA, Griffies SM, Hallberg RW, Harrison MJ, Levy H, Wittenberg AT, Phillips PJ, Zadeh N (2012) GFDL’s
379 ESM2 Global Coupled Climate-Carbon Earth System Models. Part I: Physical Formulation and Baseline Simulation
380 Characteristics. *J Clim* 25:6646–6665, DOI 10.1175/JCLI-D-11-00560.1
- 381 Dunne JP, John JG, Shevliakova S, Stouffer RJ, Krasting JP, Malyshev SL, Milly PCD, Sentman LT, Adcroft AJ, Cooke
382 W, Dunne KA, Griffies SM, Hallberg RW, Harrison MJ, Levy H, Wittenberg AT, Phillips PJ, Zadeh N (2013) GFDL’s
383 ESM2 global coupled climate-carbon earth system models. Part II: Carbon system formulation and baseline simulation
384 characteristics. *J Clim* 26(7):2247–2267, DOI 10.1175/JCLI-D-12-00150.1
- 385 Feudale L, Shukla J (2007) Role of Mediterranean SST in enhancing the European heat wave of summer 2003. *Geophys*
386 *Res Lett* 34(3):L03,811, DOI 10.1029/2006GL027991
- 387 Field CB, Intergovernmental Panel on Climate Change (2012) Managing the risks of extreme events and disasters to
388 advance climate change adaptation: special report of the Intergovernmental Panel on Climate Change. DOI 10.1017/
389 CBO9781139177245
- 390 Fischer EM, Seneviratne SI, Vidale PL, Lüthi D, Schär C (2007) Soil moisture-atmosphere interactions during the 2003
391 European summer heat wave. *J Clim* 20(20):5081–5099, DOI 10.1175/JCLI4288.1
- 392 Fouillet A, Rey G, Laurent F, Pavillon G, Bellec S, Guihenneuc-Jouyaux C, Clavel J, Jouglé E, Hémon D (2006) Excess
393 mortality related to the August 2003 heat wave in France. *Int Arch Occup Environ Health* 80(1):16–24, DOI 10.1007/
394 s00420-006-0089-4
- 395 Gómez-Navarro JJ, Werner J, Wagner S, Luterbacher J, Zorita E (2014) Establishing the skill of climate field recon-
396 struction techniques for precipitation with pseudoproxy experiments. *Clim Dyn* 45(5-6):1395–1413, DOI 10.1007/
397 s00382-014-2388-x
- 398 Hamill TM, Whitaker JS (2006) Probabilistic quantitative precipitation forecasts based on reforecast analogs: Theory and
399 application. *Mon Wea Rev* 134(11):3209–3229, DOI 10.1175/MWR3237.1

- 400 Hamill TM, Scheuerer M, Bates GT (2015) Analog Probabilistic Precipitation Forecasts Using GEFS Reforecasts and
401 Climatology-Calibrated Precipitation Analyses. *Mon Wea Rev* 143(8):3300–3309, DOI 10.1175/MWR-D-15-0004.1
- 402 Haustein K, Otto FEL, Uhe P, Schaller N (2016) Real-time extreme weather event attribution with forecast seasonal SSTs.
403 *Environ Res Lett* 11(6):1–15, DOI 10.1088/1748-9326/11/6/064006
- 404 Horton DE, Johnson NC, Singh D, Swain DL, Rajaratnam B, Diffenbaugh NS (2015) Contribution of changes in atmospheric
405 circulation patterns to extreme temperature trends. *Nature* 522(7557):465–469, DOI 10.1038/nature14550
- 406 Kalnay E, Kanamitsu M, Kistler R, Collins W, Deaven D, Gandin L, Iredell M, Saha S, White G, Woollen J, Zhu Y, Chelliah
407 M, Ebisuzaki W, Higgins W, Janowiak J, Mo KC, Ropelewski C, Wang J, Leetmaa A, Reynolds R, Jenne R, Joseph D
408 (1996) The NCEP/NCAR 40-year reanalysis project. DOI 10.1175/1520-0477(1996)077(0437:TNYRP)2.0.CO;2, arXiv:
409 1011.1669v3
- 410 Lorenz EN (1969) Atmospheric Predictability as Revealed by Naturally Occurring Analogues. *J Atmos Sci* 26(4):636–646,
411 DOI 10.1175/1520-0469(1969)26(636:APARBN)2.0.CO;2
- 412 Michelangeli PA, Vautard R, Legras B (1995) Weather Regimes: Recurrence and Quasi Stationarity. DOI 10.1175/
413 1520-0469(1995)052(1237:WRRASQ)2.0.CO;2
- 414 Peng RD, Bobb JF, Tebaldi C, McDaniel L, Bell ML, Dominici F (2011) Toward a Quantitative Estimate of Future Heat
415 Wave Mortality under Global Climate Change. *Environ Health Perspect* (May), DOI 10.1289/ehp.1002430
- 416 Poli P, Hersbach H, Dee DP, Berrisford P, Simmons AJ, Vitart F, Laloyaux P, Tan DGH, Peubey C, Th  paut JN, Tr  molet
417 Y, H  lm EV, Bonavita M, Isaksen I, Fisher M (2016) ERA-20C: An Atmospheric Reanalysis of the Twentieth Century.
418 *J Clim* 29(11):4083–4097, DOI 10.1175/JCLI-D-15-0556.1
- 419 Portela A, Castro M (1996) Summer thermal lows in the Iberian peninsula: A three-dimensional simulation. *Quat J Roy
420 Met Soc* 122(1), DOI 10.1002/qj.49712252902
- 421 Quesada B, Vautard R, Yiou P, Hirschi M, Seneviratne SI (2012) Asymmetric European summer heat predictability from
422 wet and dry southern winters and springs. *Nat Clim Change* 2(10):736–741, DOI 10.1038/nclimate1536
- 423 Radanovics S, Vidal JP, Sauquet E, Ben Daoud A, Bontron G (2013) Optimising predictor domains for spatially coherent
424 precipitation downscaling. *Hydrol Earth Sys Sc* 17(10):4189–4208, DOI 10.5194/hess-17-4189-2013
- 425 Rebetez M, Dupont O, Giroud M (2009) An analysis of the July 2006 heatwave extent in Europe compared to the record
426 year of 2003. *Theor Appl Climatol* 95(1-2):1–7, DOI 10.1007/s00704-007-0370-9
- 427 Russo S, Sillmann J, Fischer EM (2015) Top ten European heatwaves since 1950 and their occur-
428 rence in the future. *Environ Res Lett* 10(12):124,003, DOI 10.1088/1748-9326/10/12/124003
- 429 Schenk F, Zorita E (2012) Reconstruction of high resolution atmospheric fields for Northern Europe using analog-upscaling.
430 *Clim Past* 8(5):1681–1703, DOI 10.5194/cp-8-1681-2012
- 431 Seneviratne SI, L  thi D, Litschi M, Sch  r C (2006) Land-atmosphere coupling and climate change in Europe. *Nature*
432 443(7108):205–209, DOI 10.1038/nature05095
- 433 Seneviratne SI, Corti T, Davin EL, Hirschi M, Jaeger EB, Lehner I, Orlowsky B, Teuling AJ (2010) Investigating soil
434 moisture-climate interactions in a changing climate: A review. *Earth-Sci Rev* 99(3-4):125–161, DOI 10.1016/j.earscirev.
435 2010.02.004
- 436 Shepherd TG (2015) Climate science: The dynamics of temperature extremes. *Nature* 522(7557):425–427, DOI 10.1038/
437 522425a
- 438 Shepherd TG (2016) A Common Framework for Approaches to Extreme Event Attribution. *Current Climate Change
439 Report* 2:28–38, DOI 10.1007/s40641-016-0033-y
- 440 St  fanon M, Drobinski P, D’Andrea F, De Noblet-Ducoudr   N (2012) Effects of interactive vegetation phenology on the
441 2003 summer heat waves. *J Geophys Res Atmospheres* 117(24):1–15, DOI 10.1029/2012JD018187
- 442 Sutton RT, Hodson DLR (2005) Atlantic Ocean Forcing of North American and European Summer Climate. *Science*
443 309(5731):115–118, DOI 10.1126/science.1109496
- 444 Tandeo P, Ailliot P, Ruiz J, Hannart A, Chapron B, Easton R, Fablet R (2015) Combining analog method and ensemble
445 data assimilation: application to the Lorenz-63 chaotic system. *Machine Learning and Data Mining Approaches to
446 Climate Science* pp 3–12, DOI 10.1007/978-3-319-17220-0_1
- 447 Taylor KE, Stouffer RJ, Meehl Ga (2012) An Overview of CMIP5 and the Experiment Design. *Bull Amer Met Soc*
448 93(4):485–498, DOI 10.1175/BAMS-D-11-00094.1
- 449 Toth Z (1991a) Estimation of Atmospheric Predictability by Circulation Analogs. *Mon Wea Rev* 119(1):65–72
- 450 Toth Z (1991b) Intercomparison of circulation similarity measures. DOI 10.1175/1520-0493(1991)119(0055:IOCSM)2.0.CO;
451 2
- 452 Trenberth KE, Fasullo JT, Shepherd TG (2015) Attribution of climate extreme events. *Nat Clim Change* 5(August):725–
453 730, DOI 10.1038/nclimate2657
- 454 Turco M, Quintana Segu   P, Llasat MC, Herrera S, Guti  rrez JM (2011) Testing MOS precipitation downscaling for
455 ENSEMBLES regional climate models over Spain. *J Geophys Res* 116:D18,109, DOI 10.1029/2011JD016166
- 456 Van Den Dool H (2007) *Empirical Methods in Short-Term Climate Prediction*. Oxford University Press, Oxford

- 457 Vanvyve E, Monache LD, Monaghan AJ, Pinto JO (2015) Wind resource estimates with an analog ensemble approach.
458 Renewable Energy 74:761–773, DOI <http://dx.doi.org/10.1016/j.renene.2014.08.060>
- 459 Vautard R (1990) Multiple Weather Regimes over the North Atlantic: Analysis of Precursors and Successors. *Mon Wea*
460 *Rev* 118, DOI 10.1175/1520-0493(1990)118<2056:MWROTN>2.0.CO;2
- 461 Yiou P (2014) AnaWEGE: A weather generator based on analogues of atmospheric circulation. *Geosci Model Dev* 7:531–
462 543, DOI 10.5194/gmd-7-531-2014
- 463 Yiou P, Nogaj M (2004) Extreme climatic events and weather regimes over the North Atlantic: When and where? *Geophys*
464 *Res Lett* 31:1–4, DOI 10.1029/2003GL019119
- 465 Yiou P, Salameh T, Drobinski P, Menut L, Vautard R, Vrac M (2012) Ensemble reconstruction of the atmospheric column
466 from surface pressure using analogues. *Clim Dyn* 41(5-6):1333–1344, DOI 10.1007/s00382-012-1626-3
- 467 Yiou P, Boichu M, Vautard R, Vrac M, Jourdain S, Garnier E, Fluteau F, Menut L (2014) Ensemble meteorological
468 reconstruction using circulation analogues of 1781–1785. *Clim Past* 10(2):797–809, DOI 10.5194/cp-10-797-2014
- 469 Zorita E, von Storch H (1999) The analog method as a simple statistical downscaling technique: Comparison with more
470 complicated methods. *J Clim* 12(8):2474–2489, DOI 10.1175/1520-0442(1999)012<2474:TAMAAS>2.0.CO;2

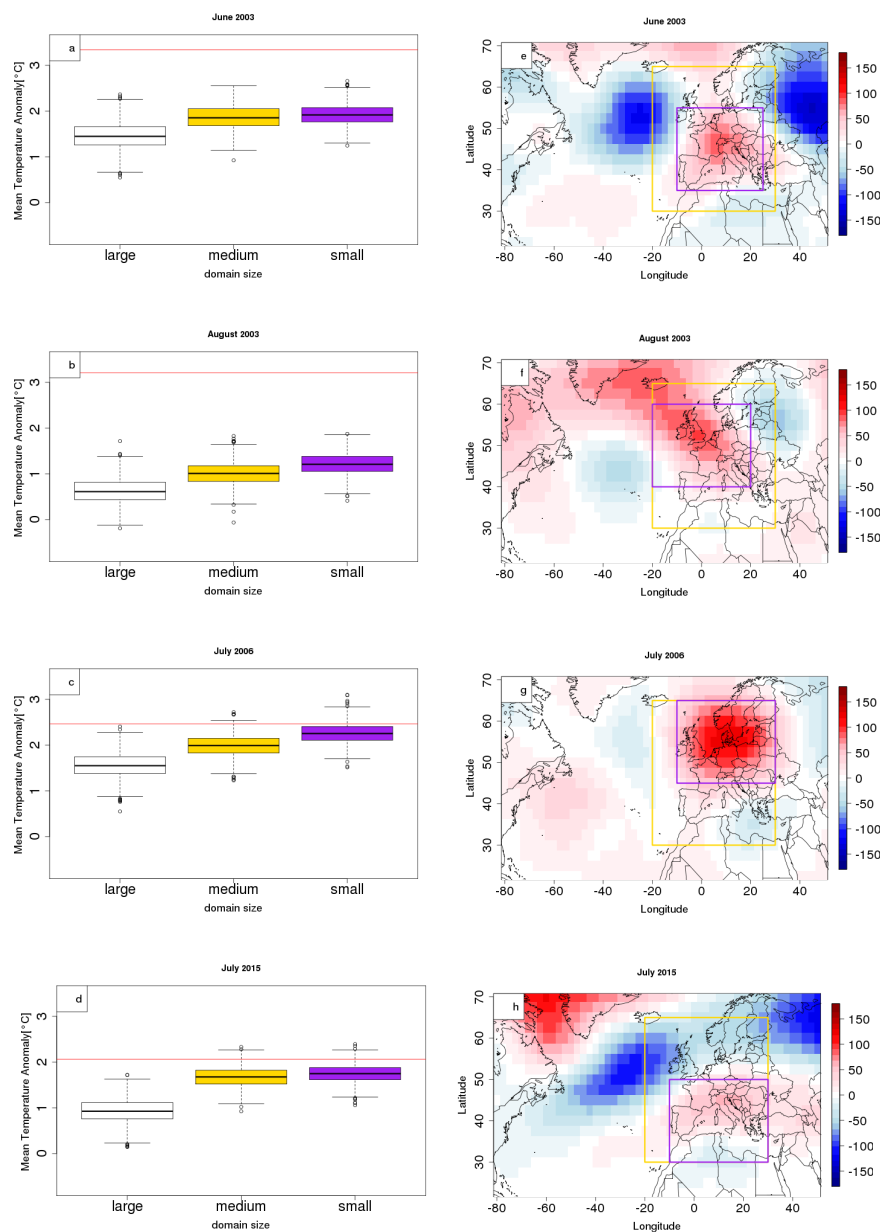


Fig. 5: Dependence of the probability density of uchronic temperature anomalies on the size of the domain. The maps on the right column represent the detrended Z500 monthly anomaly (m). The purple rectangles indicate the smallest zones of computation of flow analogues. The golden rectangles indicate the medium zone of computation of flow analogues. The large zone is the whole map. The boxplots of the left column display the distribution of the 1000 uchronic monthly detrended temperature constituted from randomly picked analogues. The color of the boxplot corresponds to the color of the rectangle delineating the region on which the analogues are computed. The red lines on the left hand side of the figure represent the observed detrended temperature of the case studies, from top to bottom : June 2003, August 2003, July 2006, July 2015.

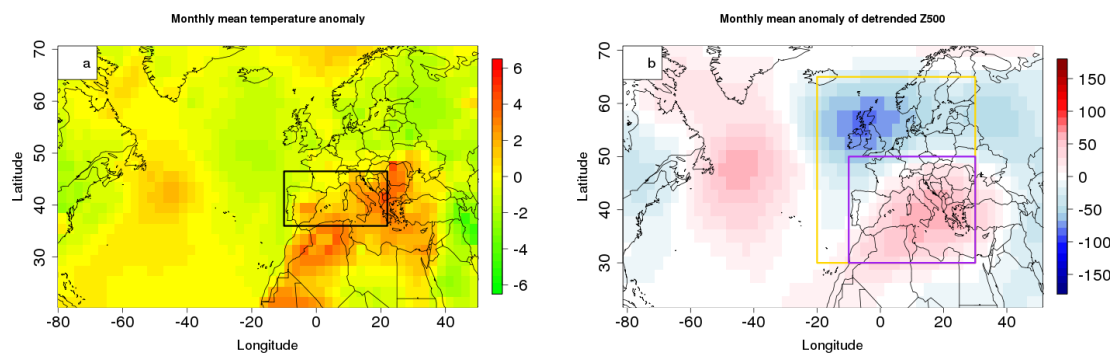


Fig. 6: Temperature anomaly (a) and Z500 anomaly (m) (b) of a July month from GFDL-ESM2M CMIP5 pre-industrial control run similar to July 2015.

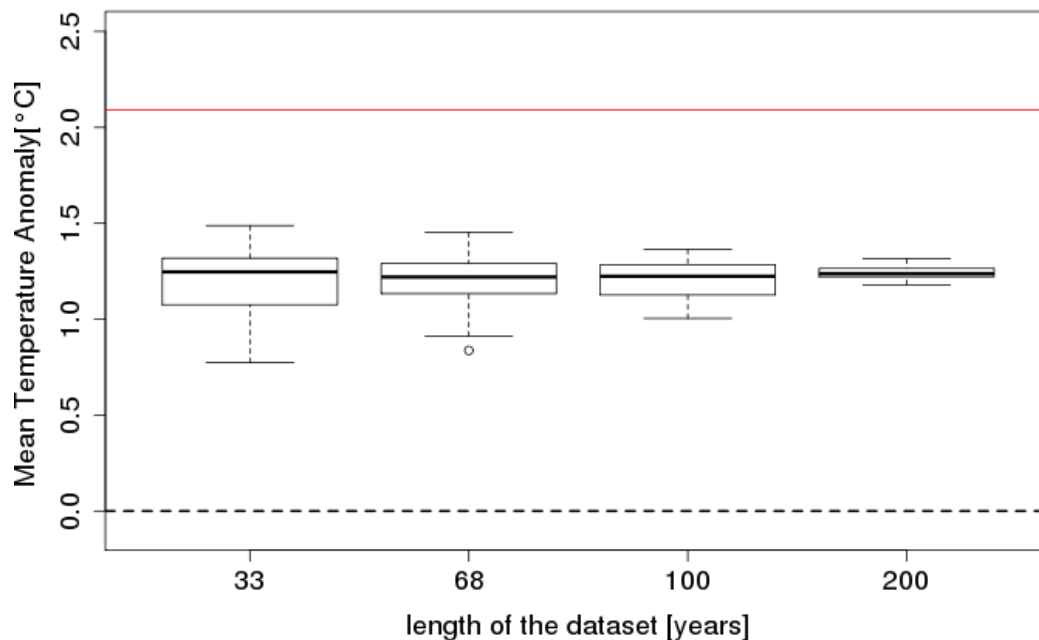


Fig. 7: Sensitivity to interdecadal variability depending on the length of the dataset. Distributions of the mean temperature of analogues generated distributions of temperature for 60 different subsets of varying sizes (33, 68, 100, or 200 years) from a 500 years long pre-industrial control run (model GFDL-ESM2M) for the small domain of analogues computation.

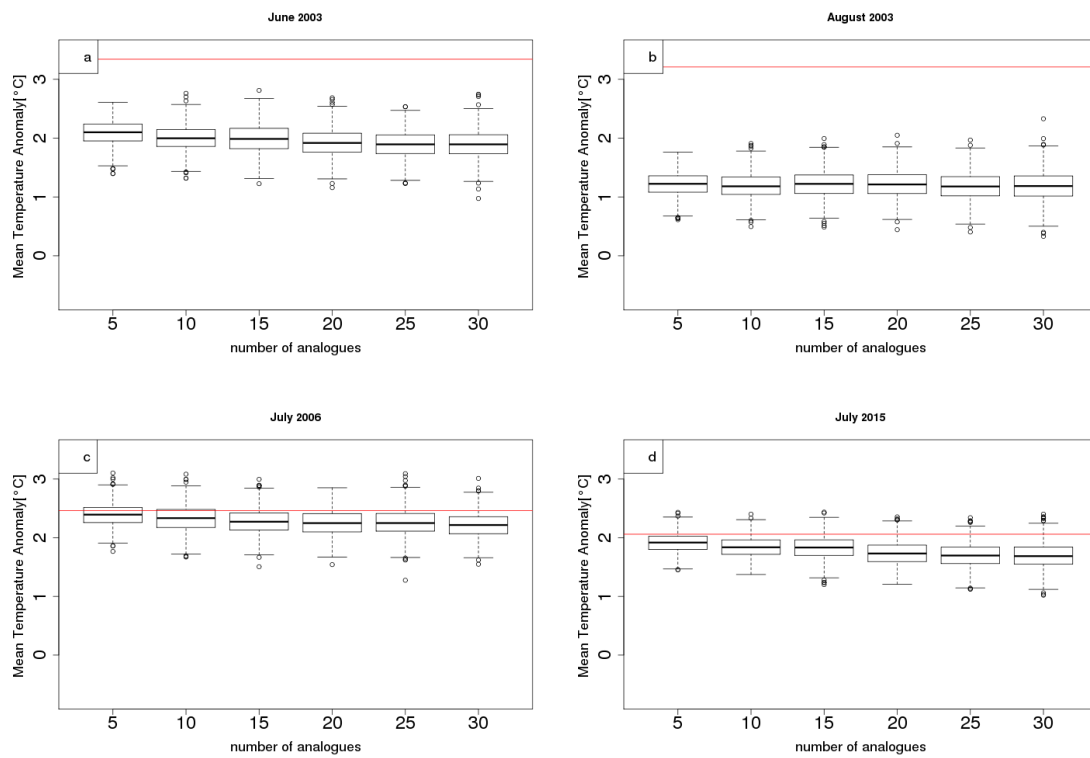


Fig. 8: Dependence of the probability density to the number of analogues. Difference between analogues generated distributions calculated using different numbers of analogues for each case study: June 2003 (a), August 2003 (b), July 2007 (c), July 2015 (d). The red line represents the observed detrended anomaly of the event.

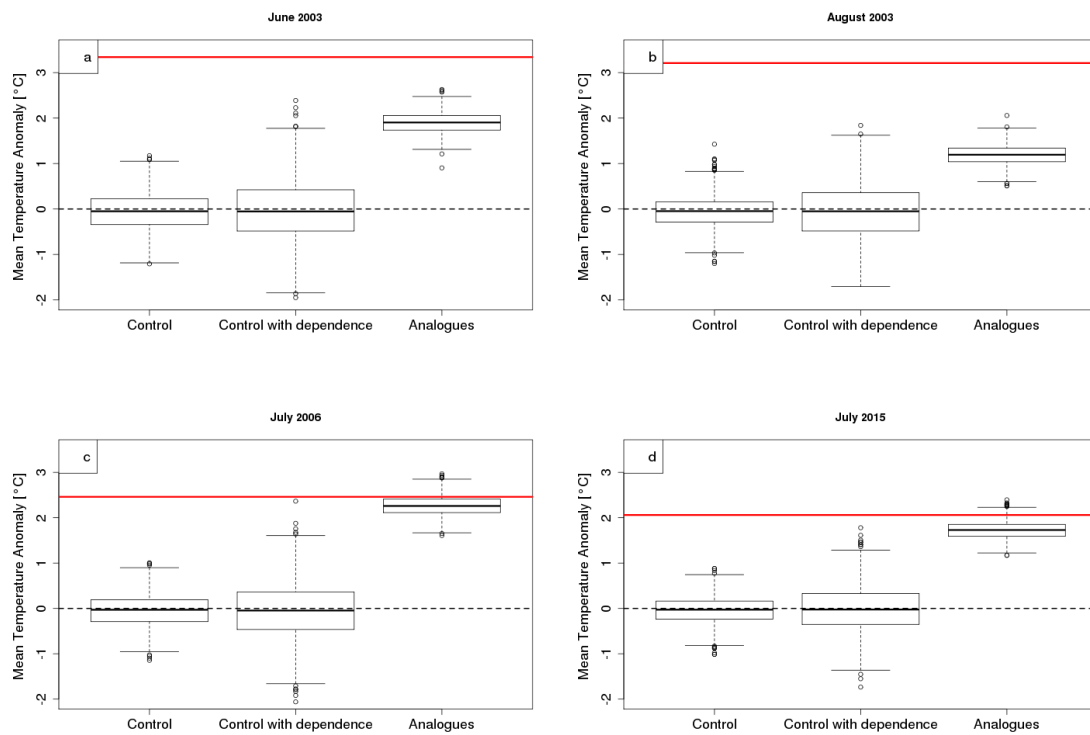


Fig. 9: Probability distributions of detrended monthly temperatures reconstructed using random days (left boxplot of each subfigure), random days picked every three days (middle boxplot of each subfigure) and analogues (right boxplot of each subfigure) for each case study: June 2003 (a), August 2003 (b), July 2007 (c), July 2015 (d). The red line represents the observed detrended anomaly of the event.

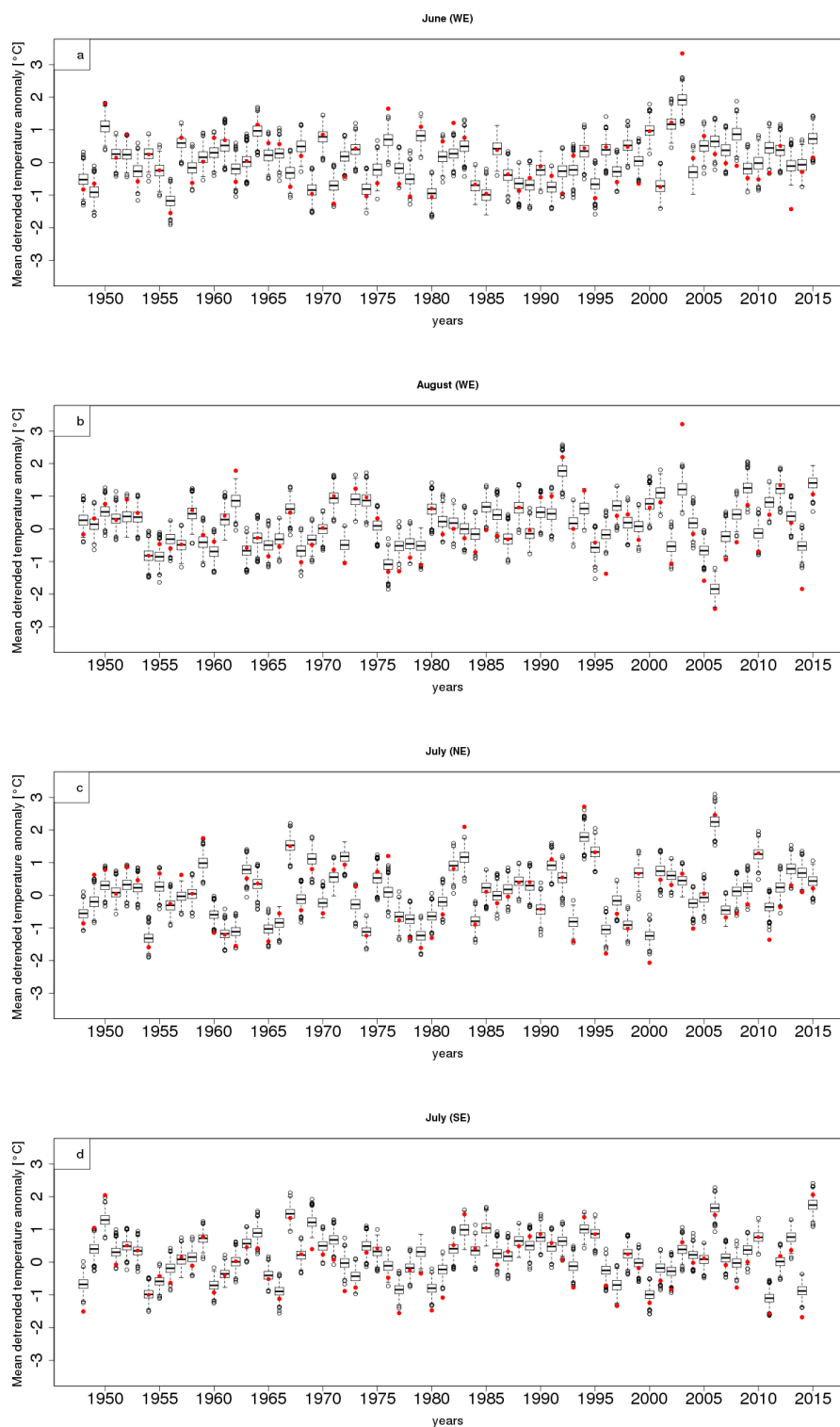


Fig. 10: Evolution of the detrended temperature distributions for all the months of June in Western Europe (a), August in Western Europe (b), July in Northern Europe (c) and July in Southern Europe (d). The regions are displayed in figure 1. The red dots correspond to the observed detrended temperature anomaly for each year.